The Journal of Experimental Biology 214, 487-500

doi:10.1242/jeb.051284

RESEARCH ARTICLE

The underwater photic environment of Cape Maclear, Lake Malawi: comparison between rock- and sand-bottom habitats and implications for cichlid fish vision

Shai Sabbah[1], Suzanne M. Gray[1,2], Emmanuel S. Boss[3], James M. Fraser[4], Richard Zatha[5] and Craig W. Hawryshyn[1,*]

[1]Department of Biology, Queen's University, 116 Barrie Street, Kingston, ON K7L 3N6, Canada, [2]Department of Biology, McGill University, 1205 Docteur Penfield, Montreal, QC H3A 1B1, Canada, [3]School of Marine Sciences, University of Maine, 5741 Libby Hall, Orono, ME 04469, USA, [4]Department of Physics, Engineering Physics and Astronomy, Queen's University, Kingston, ON K7L 3N6, Canada and [5]Department of Biology, University of Malawi, Zomba, PO BOX 278, Malawi

*Author for correspondence (craig.hawryshyn@queensu.ca)

Accepted 20 October 2010

SUMMARY

Lake Malawi boasts the highest diversity of freshwater fishes in the world. Nearshore sites are categorized according to their bottom substrate, rock or sand, and these habitats host divergent assemblages of cichlid fishes. Sexual selection driven by mate choice in cichlids led to spectacular diversification in male nuptial coloration. This suggests that the spectral radiance contrast of fish, the main determinant of visibility under water, plays a crucial role in cichlid visual communication. This study provides the first detailed description of underwater irradiance, radiance and beam attenuation at selected sites representing two major habitats in Lake Malawi. These quantities are essential for estimating radiance contrast and, thus, the constraints imposed on fish body coloration. Irradiance spectra in the sand habitat were shifted to longer wavelengths compared with those in the rock habitat. Beam attenuation in the sand habitat was higher than in the rock habitat. The effects of water depth, bottom depth and proximity to the lake bottom on radiometric quantities are discussed. The radiance contrast of targets exhibiting diffused and spectrally uniform reflectance depended on habitat type in deep water but not in shallow water. In deep water, radiance contrast of such targets was maximal at long wavelengths in the sand habitat and at short wavelengths in the rock habitat. Thus, to achieve conspicuousness, color patterns of rock- and sand-dwelling cichlids would be restricted to short and long wavelengths, respectively. This study provides a useful platform for the examination of cichlid visual communication.

Supplementary material available online at http://jeb.biologists.org/cgi/content/full/214/3/487/DC1

Key words: visibility, beam attenuation, body coloration, radiance contrast, spectral irradiance, visual communication.

INTRODUCTION

"Meaningful analysis of visual functions in nature requires precise data on the photic environment" (McFarland and Munz, 1975). Lake Malawi contains one of the most diverse fish assemblages in the world, yet its photic environment has not been comprehensively described [for selected radiometric data see Dalton et al. and Hofmann et al. (Dalton et al., 2010; Hofmann et al., 2009)]. It is essential to characterize the underwater photic environment in order to understand mechanisms of visual communication, visually mediated behavior and the visual ecology of the remarkably diverse cichlid fishes of Lake Malawi.

The spectral distribution of radiance contrast is the main determinant of the visibility of objects underwater (Duntley, 1962; Duntley, 1963; Lythgoe, 1968). The radiance contrast of an object depends on the radiance reflected from the object and the radiance of the object's background. The radiance reflected from the object depends on the spectral reflectance of the object and the spectral irradiance illuminating it. Therefore, characterizing the spectral irradiance illuminating an object and the background radiance against which the object is viewed is a prerequisite for estimation of the radiance contrast of any submerged object. The radiance contrast of an object also depends on the distance between the object and the viewer, as the radiance arriving from the object attenuates with distance according to the spectral beam attenuation coefficient. These three quantities – spectral irradiance, spectral radiance and spectral beam attenuation coefficient – and their distribution in space are the focus of the current study. We used these radiometric quantities to understand the visibility of underwater targets and examine the implications for fish vision.

Tropical Lake Malawi is the southernmost of the East African Rift Valley lakes (9°30′–14°30′S, 33°50′–35°20′E). It is 560 km long, 40–70 km wide and 22,490 km^2 in area, with a terrestrial watershed of 75,300 km^2 and a maximum depth of 700 m. Because of its high transparency and low nutrient concentration in the upper layer (Bootsma and Hecky, 2003), the lake is considered oligotrophic. Seventy percent of Lake Malawi coastline consists, generally, of sloping sandy beaches, vegetated areas and swamp. The remaining coastline is composed of steep rocky shores. The bottom of the lake is sandy (Halfman and Scholz, 1993; Pilskaln and Johnson, 1991) and, generally, rocky zones give way to sandy plains (Ribbink et al., 1983). Therefore, nearshore rocky sites differ in the depth at which a transition from rock- to sand-bottom occurs, and thus are generally divided according to their bottom substrate, into rock habitats and sand habitats, each type hosting a distinct assemblage of fish.

With respect to fish, Lake Malawi is the most species-rich lake worldwide. Approximately 1000 cichlid fish species inhabit Lake

Malawi (Fryer and Iles, 1972; Salzburger, 2009) compared with approximately 140 in the North American Great Lakes (Scott and Crossman, 1973). Lake Malawi cichlids are often grouped into two main clades: rock-dwellers (mbuna) and sand-dwellers. Adaptation to the rock and sand habitats resulted in the divergence of many morphological and behavioral characteristics including body shape, trophic morphology, body color patterning and reproductive behavior (Fryer and Iles, 1972; Ribbink et al., 1983). That vision may play a crucial role in guiding cichlid communication and speciation (Carleton et al., 2006; Couldridge and Alexander, 2002; Jordan et al., 2003; Seehausen et al., 2008; Seehausen and van Alphen, 1998; Seehausen et al., 1997) emphasizes the need for studies that examine the constraints imposed by the underwater photic environment on the color of body patterns and visual abilities of Lake Malawi cichlids.

In this study, we measure key facets of the photic environment and apply this information to understanding the principal factors that affect fish vision. Here we examine: (1) the underwater spectral irradiance, spectral radiance and spectral beam attenuation coefficient in the two major habitats in Lake Malawi; (2) the effects of water depth, bottom depth and proximity to bottom on the radiometric quantities and beam attenuation; and (3) the constraints imposed on body color patterns of cichlids by the photic environment of the two major habitats in Lake Malawi.

MATERIALS AND METHODS

Study site

This study was conducted from 23 to 29 July 2008 at two nearshore sites around Cape Maclear on the northwestern part of the Nankumba Peninsula, Lake Malawi (part of Lake Malawi National Park). The first sampling site, Otter Point (14°02′21.02″S, 34°49′20.33″E), is exposed to wind and wave action (Fryer and Iles, 1972; Ribbink et al., 1983) and exhibited a rock–sand transition at a depth of 15 m (henceforth ‘rock habitat’). Mawlamba, the second sampling site, on the northern shore of Thumbi West Island (14°01′05.92″S, 34°48′59.91″E), is a small sheltered bay where the rock–sand transition depth was 3 m (henceforth ‘sand habitat’). Thumbi West Island is relatively heavily forested and is not inhabited.

Spectral irradiance and radiance measurements

To characterize the photic conditions encountered by fish occupying different positions within the two habitats, spectral irradiance was measured along three measurement profiles, designed to examine the effect of different environmental factors on the photic environment (Fig. 1). Lake Malawi cichlids are typically found in the upper 10–20 m of the water column (Konings, 1995; Ribbink et al., 1983); therefore, irradiance was measured down to a depth of 15 m. Profile 1 was designed to examine the effect of water depth (four to six points between 1 and 15 m of depth) on the photic environment. Profile 2 was designed to evaluate the effect of bottom depth on the photic environment while maintaining a fixed distance of 1 m above the bottom (five points between 3 and 15 m of depth). Profile 3 was designed to examine the effect of distance from the bottom on the photic environment while swimming away from shore at a constant depth of 5 m (four to six points between 1 and 10 m away from the bottom). However, bottom depth and distance from shore correlate, thus their effects could not be separated. Irradiance was measured at three cardinal sampling orientations at each point along the measurement profiles: downwelling (E_d; the irradiance probe pointing upwards), upwelling (E_u; probe pointing downwards) and sidewelling (E_h; probe pointing a horizontal line of sight). Three

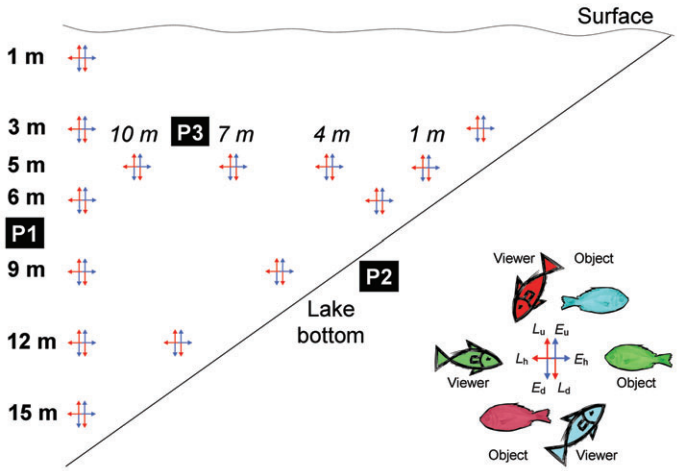

Fig. 1. A schematic representation of the measurement profiles along which spectral irradiance (blue) and spectral radiance (red) were measured. Measurements of downwelling (arrows pointing downward), sidewelling (arrows pointing sideward) and upwelling (arrows pointing upward) were acquired along the three profiles (P1–P3). Sidewelling irradiance measurements were obtained with the probe pointing offshore whereas sidewelling radiance measurements were taken with the probe pointing inshore. The bottom depth below P1 was 16 m. The depth of each of the measurement points along P1 and P2 is indicated. The distance away from the bottom is indicated next to each of the measurement points along P3 (italics). Measurements along P2 were taken at a constant distance of 1 m away from the lake bottom. The inset demonstrates how the irradiance (E) and radiance (L) at different sampling orientations correspond to the irradiance that impinges on an object and the background radiance against which the object is viewed. For example, viewing an object from above, the object is illuminated by the downwelling irradiance (E_d; downward-pointing blue arrow) and is viewed against the upwelling radiance background (L_u; upward-pointing red arrow). The viewers are positioned differently, depending on their viewing orientation. Each object–viewer pair is color coded; for instance, the red viewer is looking at the red object and the green viewer is looking at the green object.

consecutive spectra were acquired at each sampling orientation. For each spectrum collected, we calculated the mean irradiance across the entire wavelength range. We used these three mean irradiance values, associated with the three irradiance spectra, to select the spectrum associated with the intermediate mean irradiance value. This spectrum was used in further analysis.

In addition to irradiance, the underwater spectral radiance was also measured along measurement profiles 2 and 3 at the three cardinal sampling orientations described. However, while sidewelling irradiance measurements were made with the probe pointing offshore, sidewelling radiance measurements were taken with the probe pointing inshore (see Results for clarification). Measurements along profiles 2 and 3 were taken on the same day whereas those along profile 1 were obtained on a separate day. All measurements were made at approximately noon, corresponding to a solar zenith angle of 33–50 deg during July and August 2008 (except the radiance measurements for profiles 2 and 3 in the sand habitat, during which solar zenith angle ranged from 52 to 68 deg). Table 1 summarizes the locations, dates, times and solar zenith angles at which the various measurement profiles were acquired. Measurements taken while the sun was obscured by clouds were removed from analysis. Additionally, prior to each measurement session, downwelling irradiance and radiance were measured just above the water surface.

Radiometric data acquisition

Irradiance was measured using a thermoelectrically cooled spectroradiometer (QE65000, Ocean Optics, Dunedin, FL, USA) connected to a 30 m optical fiber (ZPK600-30-UV/VIS, Ocean Optics) that was fitted with a cosine corrector (CC-3-UV, Ocean Optics). To measure radiance, the cosine corrector was replaced with an acceptance angle restrictor with an acceptance cone of 10 deg. The spectroradiometer configuration included a 1024×58-element square silicon CCD array with a 25 μm slit, and a variable blaze wavelength grating (HC-1, groove density=300 mm^{-1}, Ocean Optics), resulting in an effective spectral resolution of 1.9 nm (FWHM) between 200 and 950 nm. For all measurements, the spectroradiometer's integration time and the number of averaged spectra were adjusted so that sampling time was longer than 2 s. This allowed us to average irradiance/radiance fluctuations induced by surface waves and to obtain the most stable readings. The spectroradiometer setup was calibrated for absolute irradiance/radiance prior to each measurement day using a NIST calibrated halogen–deuterium dual light source (200–1000 nm, DH-2000-CAL, Ocean Optics). A SCUBA diver held the irradiance probe and maintained position at discrete points along the measurement profiles while readings were acquired and saved on a laptop computer located on a boat that was positioned as far as possible from the diver and never between the diver and the sun, to prevent shading.

Analysis of irradiance and radiance spectra

While the individual irradiance and radiance spectra were highly informative and easy to understand, a means of data reduction was implemented, in order to compare spectra and to examine the effects of environmental factors on the measured spectra. First, to quantify the absolute quanta delivered at each measurement point, the area under each spectral curve was integrated between 300 and 750 nm to give irradiance (photons cm^{-2} s^{-1}) or radiance (photons cm^{-2} sr^{-1} s^{-1}). This spectral range was chosen to conform to the spectral range that may be relevant for fish vision (e.g. Hawryshyn and Harosi, 1994; Losey et al., 2003; Parry et al., 2005). To characterize the spectral distribution of irradiance/radiance spectra, we calculated the λP_{50} – the wavelength that halves the total number of photons between 300 and 750 nm (McFarland and Munz, 1975). The λP_{50} value specifies that wavelength about which quanta are likely to be most abundant. The longer the λP_{50}, the more the spectrum is shifted to longer wavelengths. As a measure of the spectrum bandwidth, we calculated the λP_{25} and λP_{75} values (which are comparable to the cumulative frequency distribution at the 25th and 75th percentiles, respectively) and the wavelength interval enclosed by the two, $\Delta\lambda=\lambda P_{75}-\lambda P_{25}$. The larger the $\Delta\lambda$, the larger the bandwidth of the spectrum. Such an index is appropriate for underwater irradiance and radiance spectra where spectral distribution is unimodal. For several spectra, especially those acquired at greater depths, the irradiance/radiance levels at both edges of the spectrum were considered to be too low to be reliable. These unreliable sections of the spectrum were truncated for further analyses.

The localized spectral attenuation coefficient of downwelling irradiance, $K_d(\lambda)$, was calculated following Kirk (Kirk, 1981) and Mobley (Mobley, 1994) as:

$$K_d(\lambda) = \frac{1}{z}\ln[E_{dz}(\lambda) / E_{d0}(\lambda)], \quad (1)$$

where E_{dz} is the downwelling irradiance at depth z and E_{d0} is the downwelling irradiance at zero depth (or just above the water surface). In this study, z was taken as the deepest measurement point, 15 m. The calculation of $K_d(\lambda)$ was restricted to the spectral range 320–700 nm because of the insufficient signal for the 15 m measurement point.

Spectral beam attenuation measurements

To characterize the beam attenuation coefficient at different positions in the two habitats studied, water samples were collected along the three measurement profiles concurrently with the irradiance measurements. Three samples of lake water were collected at each measurement point. In order to ensure sufficient water volume, each sample of lake water included water collected by two 60 ml syringes. Analysis of water samples commenced 1 h following water collection; during the intervening time, water samples were kept in a cool and light-tight compartment.

The transmission of light through water samples was measured using a custom-built portable hyperspectral transmissometer system. This system and its performance have been described in detail elsewhere (Sabbah et al., 2010a). In short, the transmissometer system consisted of: (1) a light source (DH-2000-BAL, Ocean Optics), (2) a fiber-coupled modular spectroscopic system incorporating two identical spectrometers (Jaz, Ocean Optics) and (3) a custom-built transmissometer. The light source consisted of two lamp types – tungsten-halogen and deuterium – providing a balanced output between 200 and 1000 nm. Light was collected simultaneously by both spectrometers. One spectrometer was designated as the signal channel and the other as the reference channel. The reference channel was used to monitor the source output power and to correct the signal reading accordingly. Each of the spectrometers had a 2048-element linear silicon CCD array and was configured with a 50 μm slit and a grating (groove density=600 mm^{-1}; blaze wavelength=400 nm; grating #2, Ocean Optics), resulting in an optical resolution of 2.06 nm. The transmissometer's optical design followed the traditional collimated-beam design (Voss and Austin, 1993) with a 25 cm path length (positioned vertically) and an in-water acceptance angle of

Table 1. Location, date, time and solar zenith angle at which measurement profiles were obtained from two sites in Lake Malawi

Habitat	Quantity	Profile	Date (July 2008)	Local time (GMT + 02:00 h)	Solar zenith angle (deg)
Rock	Irradiance	1	23	10:57–11:49	36–34
		2	25	10:46–11:57	36–34
		3	25	12:30–13:21	35–41
	Radiance	2	26	11:32–12:13	34
		3	26	12:28–12:55	35–38
Sand	Irradiance	1	29	11:24–12:10	33
		2	28	12:32–14:21	34–50
		3	28		
	Radiance	2	26	14:31–15:51	52–68
		3	26		

0.55–0.59 deg across the 300–750 nm spectral range. The raw precision of the system was determined to average 0.012 m^{-1} across the spectrum (Sabbah et al., 2010a). The transmissometer had two openings fitted with valves through which water samples were injected.

Pure water calibration was performed prior to each measurement session in order to determine the offset values of attenuation that result in a zero reading with optically pure water. As a pure water standard, we used water that was purified and filtered using a Milli-Q water purification system (Milli-Q Synthesis-10, Millipore, Billerica, MA, USA), combining ultraviolet photo-oxidation and ultra-filtration, and resulting in pure water with nominal resistance of 18.2 MΩ cm and low levels of dissolved organics. Three water calibration trials were performed to confirm the offset accuracy. Typically, a standard deviation of 0.01 m^{-1} (ranging 0.0005–0.04 m^{-1} across the spectrum) across the three water calibration trials was achieved. Water temperature was measured at a resolution of 0.1°C using an electronic handheld thermometer, and water salinity was measured at a resolution of ±1‰ using a mechanical handheld refractometer. In this study, the temperature of the lake water samples ranged between 21 and 25°C whereas the salinity of all water samples was zero.

An identical measuring procedure of the transmission of light was applied to both pure water calibration and natural water transmission measurement. Water samples were injected through the flow tube by continuously pushing water from the two syringes (filled at the same point along a given measuring profile) at a flow rate of ~0.1 liters min^{-1}, during which transmission readings were collected. This flow rate was high enough to reduce particle settlement but not high enough to induce the formation of air bubbles. All processing procedures, including correction of the measured attenuation for the effects of temperature and salinity on pure water scattering, absorption and refractive index, are specified in Sabbah et al. (Sabbah et al., 2010a).

To evaluate the effect of water depth, bottom depth and proximity to the bottom on the beam attenuation, the change in attenuation due to dissolved and particulate matter at the middle of the spectrum, 525 nm, $c_{pg}(525)$, was examined. The total spectral beam attenuation, $c_t(\lambda)$, was calculated as the sum of the attenuation of optically pure water and the measured attenuation due to dissolved and particulate matter, $c_{pg}(\lambda)$. The attenuation of pure water was calculated as the sum of pure water absorption (Pope and Fry, 1997; Z. Lu, 2006) (merging at 400 nm) and scattering (Zhang et al., 2009). Total beam attenuation data was limited to 300–727 nm by the spectral range of available data for pure water attenuation.

Spectral radiance contrast calculation

To estimate the radiance contrast (between fish and the background) for fish that occupy different positions in the sand and rock habitats (horizontal line of sight), the radiance contrast of various targets was calculated following Duntley (Duntley, 1962) and Lythgoe (Lythgoe, 1968). The spectral radiance of a vertically oriented diffusely reflecting target at zero distance from the viewer, $L_{t0}(\lambda)$ (photons cm^{-2} sr^{-1} s^{-1}), was calculated as:

$$L_{t0}(\lambda) = \frac{R_t(\lambda) \cdot E_h(\lambda)}{\pi} , \quad (2)$$

where $R_t(\lambda)$is the spectral reflectance of the target (ranges from 0 to 1) and $E_h(\lambda)$ (photons cm^{-2} s^{-1}) is the spectral irradiance measured at a horizontal line of sight. The spectral radiance of the target when positioned at a distance z from the viewer, $L_{tz}(\lambda)$ (photons cm^{-2} sr^{-1} s^{-1}), was then calculated following Duntley (Duntley, 1962):

$$L_{tz}(\lambda) = \left[L_{t0}(\lambda) e^{-c_t(\lambda) z} \right] + L_h(\lambda) \left[1 - e^{-c_t(\lambda) z} \right] , \quad (3)$$

where the first term on the right describes the attenuation of image-forming radiance and the second term represents the gain of non-image-forming radiance that scatters into the eye (veiling light), $c_t(\lambda)$ (m^{-1}) is the total spectral beam attenuation coefficient and $L_h(\lambda)$ (photons cm^{-2} sr^{-1} s^{-1}) is the spectral radiance of water background at a horizontal line of sight. Finally, the radiance contrast of the target against the water background at a horizontal line of sight as perceived by a viewer at z distance away, $C_{tz}(\lambda)$, was calculated as (Lythgoe, 1968):

$$C_{tz}(\lambda) = \frac{L_{tz}(\lambda) - L_h(\lambda)}{L_h(\lambda)} . \quad (4)$$

It is important to note that the conspicuousness of animals can also be examined using a somewhat different approach. Instead of estimating the radiance contrast of the animal, the conspicuousness of colors can be evaluated as their Euclidian distance in color space from environmental radiance backgrounds and from other colors on the same animal (Endler et al., 2005; Kelber et al., 2003; Marshall, 2000; Vorobyev et al., 1998). In a previous study, the conspicuousness of female and male rock-dwelling cichlids was modeled and the selective forces shaping this conspicuousness were assessed (Dalton et al., 2010).

Statistical analysis

Prior to performing statistical analyses, normality of all data was confirmed using the Kolmogorov-Smirnov test, and homogeneity of variance was confirmed using the Cochran's *C*-test (Underwood, 1997). We investigated the effects of habitat and sampling orientation on the λP_{50} and $\Delta\lambda$ of irradiance and radiance using separate two-way ANOVAs with habitat type (sand and rock) and sampling orientation (E_d, E_h and E_u) as the main factors, plus the interaction between habitat and sampling orientation. *Post hoc* analyses were performed using Tukey's honestly significant difference (HSD) test. Profile was not taken as a main factor in the ANOVAs as measurement points along each profile corresponded to a gradient of various environmental factors. Thus, all profiles included measurement points close to surface, close to the bottom and in the water column. We then performed more detailed analyses examining the effect of several environmental factors on the irradiance, radiance and beam attenuation along the three measurement profiles. As a result of the limited number of data points along individual measurement profiles (four to six points), normality could not be assumed, and thus non-parametric statistics were used. To evaluate the effect of water depth, bottom depth and proximity to bottom on λP_{50}, $\Delta\lambda$ and $c_{pg}(525)$ along individual profiles, the Spearman correlation coefficient was calculated for each habitat and profile and, in the case of λP_{50} and $\Delta\lambda$, for each sampling orientation separately. To examine the effect of habitat type on the beam attenuation, $c_{pg}(525)$, the Mann–Whitney *U*-test was used, with habitat as a main factor. This analysis was repeated four times: once when pooling attenuation values for all profiles and three more times when examining the effect of habitat on the attenuation along each of the three profiles separately. Additionally, to compare the mean λP_{50} and $\Delta\lambda$ at different sampling orientations along each profile and for each habitat separately, the non-parametric Kruskal–Wallis analysis of variance was performed. The Wilcoxon matched pairs test was used to compare the λP_{50} and $\Delta\lambda$ values of irradiance with those of radiance at opposite sampling orientations,

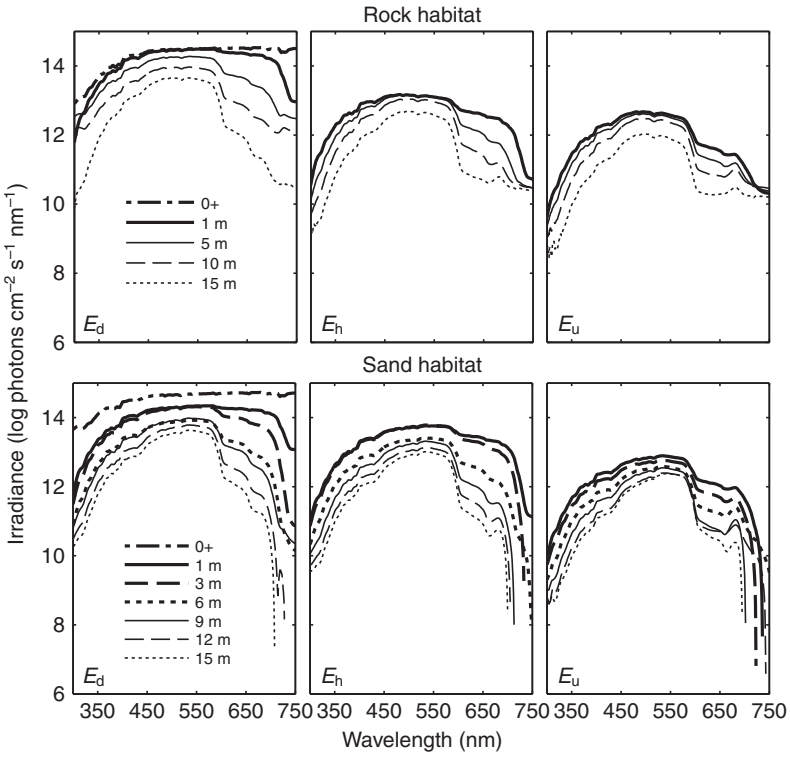

Fig. 2. Downwelling (E_d), sidewelling (E_h) and upwelling (E_u) irradiance measured along a vertical depth profile (P1) from just above the water surface (0+) down to 15 m in rock and sand habitats in Lake Malawi. Bottom depth was 16 m.

for each profile separately and with measurements from both habitats pooled. All statistical analyses were performed using STATISTICA® software (StatSoft, Tulsa, OK, USA).

RESULTS

In total, more than 350 spectral irradiance and radiance measurements were acquired in the rock and sand habitats along three measurement profiles at three sampling orientations (downwelling, sidewelling and upwelling). Concurrent with the irradiance measurements, a total of 87 lake water samples were collected along the measurement profiles and their transmission was analyzed.

Irradiance

λP_{50} and $\Delta\lambda$ indices were calculated for irradiance measurements taken along the three measurement profiles (ANOVA results and descriptive statistics are summarized in Table 2). The λP_{50} of irradiance significantly differed between habitats for all measurement profiles and sampling orientations with λP_{50} in the sand habitat being longer than that in the rock habitat. Additionally, the λP_{50} of irradiance differed significantly across sampling orientations. *Post hoc* analysis revealed that λP_{50} values of sidewelling was significantly shorter than those of downwelling and upwelling irradiance (Tukey's HSD, P=0.01 and 0.005, N=84), whereas the latter two did not differ significantly (P=0.91).

The $\Delta\lambda$ of irradiance did not differ significantly between habitats. However, it did differ significantly between sampling orientations. *Post hoc* analysis revealed that $\Delta\lambda$ of E_d was significantly larger than of E_h and E_u (Tukey's HSD, P=0.03 and 0.0002, N=84), whereas the latter two values did not differ significantly (P=0.14).

Effect of water depth on spectral irradiance

To examine the effect of water depth on irradiance, measurements were taken along a vertical profile 1 (P1; Fig. 2). Downwelling irradiance just above the water surface was relatively flat across the spectrum (300–750 nm), attaining a maximum irradiance of 5.3×10^{14} and 3.4×10^{14} photons cm^{-2} s^{-1} nm^{-1} at approximately 660 nm in the sand and rock habitats, respectively. Table 3 summarizes the total irradiance (integrated over 300–750 nm) measured just above the surface and at the minimum (1 m) and maximum (15 m) measurement depths. Total downwelling irradiance just above the water surface E_d(0+) was similar in both habitats. In both habitats, total downwelling irradiance (E_d) decreased with increasing depth where the total irradiance at 15 m corresponded to approximately 10% of that at 1 m. Total sidewelling (E_h) and upwelling (E_u) irradiance also decreased with increasing depth. See supplementary material Table S1 for total irradiance values for all measurement depths.

The spectral distribution of irradiance at the various depths differed between habitats (Figs 2, 3). The λP_{50} of E_d just above the

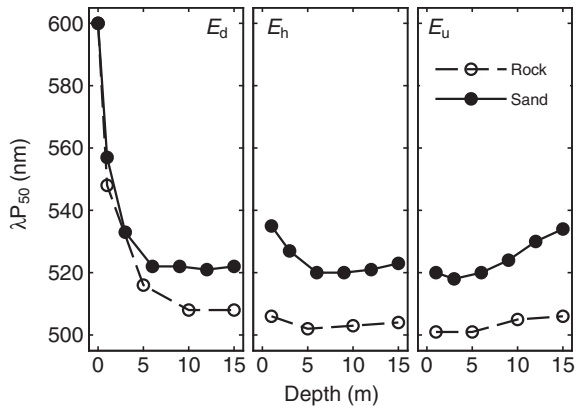

Fig. 3. The wavelength that halves the total number of photons between 300 and 750 nm (λP_{50}) of downwelling (E_d), sidewelling (E_h) and upwelling (E_u) irradiance measured along P1 in rock and sand habitats in Lake Malawi.

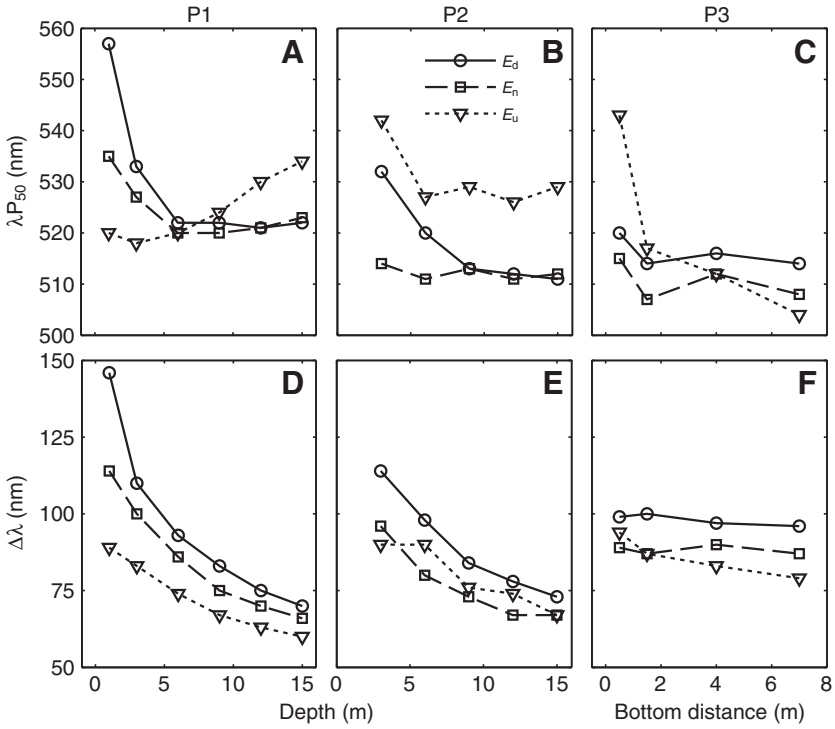

Fig. 4. λP_{50} (A–C) and spectrum bandwidth ($\Delta\lambda$) (D–F) values of downwelling (E_d), sidewelling (E_h) and upwelling (E_u) irradiance measured along P1 (sand habitat) and P2 and P3 (rock habitat) in Lake Malawi.

water surface was identical in both habitats. Underwater, however, the λP_{50} in the sand habitat was longer than that in the rock habitat at all sampling orientations. In general, the effect of water depth, as well as the effects of bottom depth and distance from the bottom, on the radiometric quantities was comparable across habitats. Hereafter, the effect of any given environmental factor will be presented for one habitat only.

In the sand habitat, λP_{50} values of both E_d and E_h shifted to shorter wavelengths with increasing depth down to approximately 6 m. In deeper water, however, λP_{50} values of E_d and E_h slightly shifted to longer wavelengths (Fig. 4A). The λP_{50} of E_u shifted to longer wavelengths with increasing depth, indicating an increase in the proportion of long wavelengths with depth. The $\Delta\lambda$ significantly decreased with depth at all sampling orientations (Fig. 4D), with the $\Delta\lambda$ of E_d and E_u being the largest and smallest, respectively. See supplementary material Table S2 for results of Spearman correlations to examine the effect of water depth and other environmental factors on irradiance.

Effect of bottom depth on spectral irradiance

Profile 2 was obtained while descending along the bottom of the lake from 3 to 15 m depth and maintaining a constant distance of 1 m above the bottom. Descending along the lake bottom in the rock habitat, the λP_{50} of E_h did not vary significantly with depth. However, the λP_{50} of E_d shifted to shorter wavelengths with increasing depth down to 9 m and then leveled off and converged with the λP_{50} of E_h. The λP_{50} of E_u shifted to shorter wavelengths down to 6 m deep and then reached a plateau (Fig. 4B). Interestingly, λP_{50} of E_u was always longer than those at the other sampling orientations (Kruskal–Wallis $H_{2,15}$=7.554, P=0.02), indicating a high proportion of long wavelengths reflected off the bottom. The $\Delta\lambda$ at all sampling orientations decreased with depth (Fig. 4E).

Effect of proximity to bottom on spectral irradiance

Profile 3 was measured while swimming away from shore at a constant water depth of 5 m. The λP_{50} and $\Delta\lambda$ of E_d did not vary significantly while swimming away from the shore, suggesting that the water column was relatively homogeneous. The λP_{50} and $\Delta\lambda$ of E_u shifted to shorter wavelengths with increasing distance from the bottom (Fig. 4C,F). However, the λP_{50} and $\Delta\lambda$ of E_h did not show a clear dependence on the proximity to the bottom (Fig. 4C).

Downwelling diffuse attenuation coefficient

The downwelling diffuse attenuation coefficient (K_d) attained maximum values at the long wavelength end of the spectrum examined, with large attenuation values also at the short wavelength end of the spectrum. The sand habitat exhibited a slightly larger diffuse attenuation, with the exception of the 550–600 nm region where attenuation in both habitats was similar (Fig. 5). The minimum attenuation was found at 502 nm in the rock habitat and 534 nm in

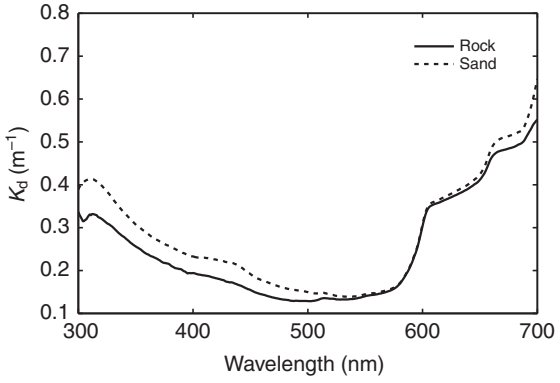

Fig. 5. The localized spectral diffuse attenuation coefficient $K_d(\lambda)$ in rock and sand habitats in Lake Malawi.

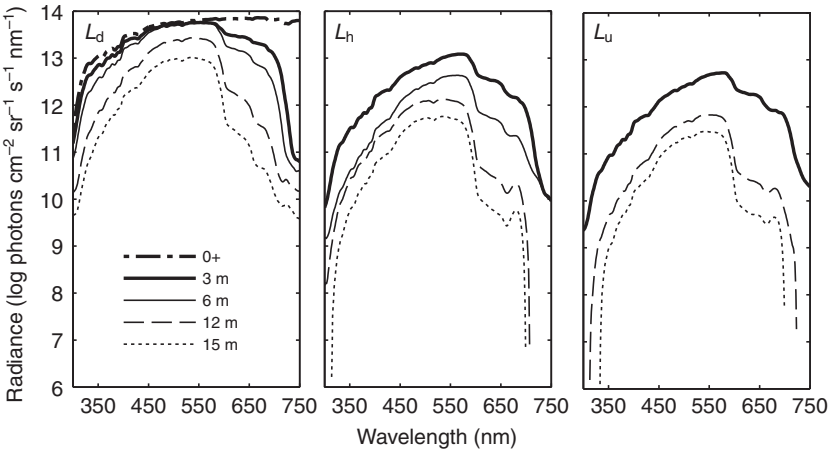

Fig. 6. Downwelling (L_d), sidewelling (L_h) and upwelling (L_u) radiance measured along the lake bottom at a constant distance of 1 m above bottom (P2), from just above the water surface (0+) down to a depth of 15 m in the sand habitat. The L_u spectrum at 6 m and all spectra at 9 m were excluded because of cloud cover during the measurement.

the sand habitat, corresponding with the differences in λP_{50} of irradiance between habitats throughout this study.

Radiance

The λP_{50} and $\Delta\lambda$ indices were calculated for radiance measurements taken along the measurement profiles 2 and 3 (ANOVA results and descriptive statistics are summarized in Table 2). The λP_{50} of radiance did not differ significantly between habitats or sampling orientations, and the $\Delta\lambda$ of radiance did not differ significantly between habitats; however, $\Delta\lambda$ values differed significantly between sampling orientations. *Post hoc* analysis revealed that the $\Delta\lambda$ of downwelling radiance was significantly larger than those of sidewelling and upwelling radiance (Tukey's HSD, P=0.004 and 0.01, N=52), whereas the latter two did not differ significantly (P=0.92).

Effect of bottom depth on spectral radiance

Radiance was measured just above the water surface and while descending along the lake bottom down to 15 m depth, at a constant distance of 1 m above the bottom (profile 2) in both habitats. As an example, Fig. 6 shows the radiance spectra acquired in the sand habitat. Total downwelling radiance just above the water surface was relatively flat across the 300–750 nm spectral range, attaining a maximum radiance of 6.5×10^{14} and 8.3×10^{14} photons cm^{-2} sr^{-1} s^{-1} nm^{-1} at approximately 680 nm in the sand and rock habitats, respectively. Table 3 summarizes the total radiance (integrated over 300–750 nm) measured just above the water surface and at the minimum (3 m) and maximum (15 m) measurement depths. In both habitats, total downwelling (L_d), sidewelling (L_h) and upwelling (L_u) radiance decreased with increasing depth. See supplementary material Table S1 for total radiance values for all measurement depths.

Measuring the spectral radiance along profile 2 in the sand habitat, the λP_{50} of L_d and L_h shifted significantly to shorter wavelengths as bottom depth increased whereas the λP_{50} of L_u did not vary significantly with bottom depth (Fig. 7A). The $\Delta\lambda$ of L_d decreased significantly with bottom depth. Although not statistically significant, the same trend was observed for L_h and L_u (Fig. 7C). The λP_{50} and $\Delta\lambda$ of radiance in the two habitats did not differ and showed a similar dependence on bottom depth (data not shown). See supplementary material Table S2 for results of Spearman correlations examining the effect of water depth and other environmental factors on radiance.

Effect of proximity to bottom on spectral radiance

Measuring the spectral radiance along profile 3 in the rock habitat, the λP_{50} of L_u shifted to shorter wavelengths with growing distance from the lake bottom (Fig. 7B). By contrast, the λP_{50} of L_h did not vary significantly with distance from the bottom. As expected, the λP_{50} of L_d did not vary with distance from the bottom (see supplementary material Table S2). The $\Delta\lambda$ of L_d was significantly larger than those for L_h and L_u (Kruskal–Wallis $H_{2,12}$=7.564, P=0.02; Fig. 7D), all decreasing with distance from the bottom down to 4 m and then leveling off. λP_{50} and $\Delta\lambda$ values measured for the sand habitat did not differ from those for the rock habitat and varied similarly with proximity to the bottom (data not shown).

Irradiance–radiance relationship

The relationship between irradiance and radiance, measured at opposite orientations, is crucial for the understanding of the visual constraints imposed on fish vision. The background against which an object is viewed is equivalent to the radiance measured in an

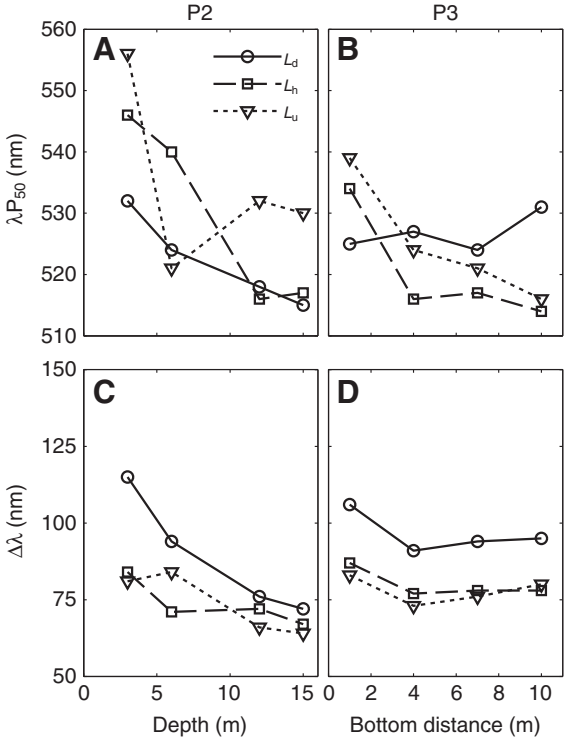

Fig. 7. λP_{50} (A,B) and $\Delta\lambda$ (C,D) of downwelling (L_d), sidewelling (L_h) and upwelling (L_u) radiance measured along P2 (sand habitat) and P3 (rock habitat) in Lake Malawi.

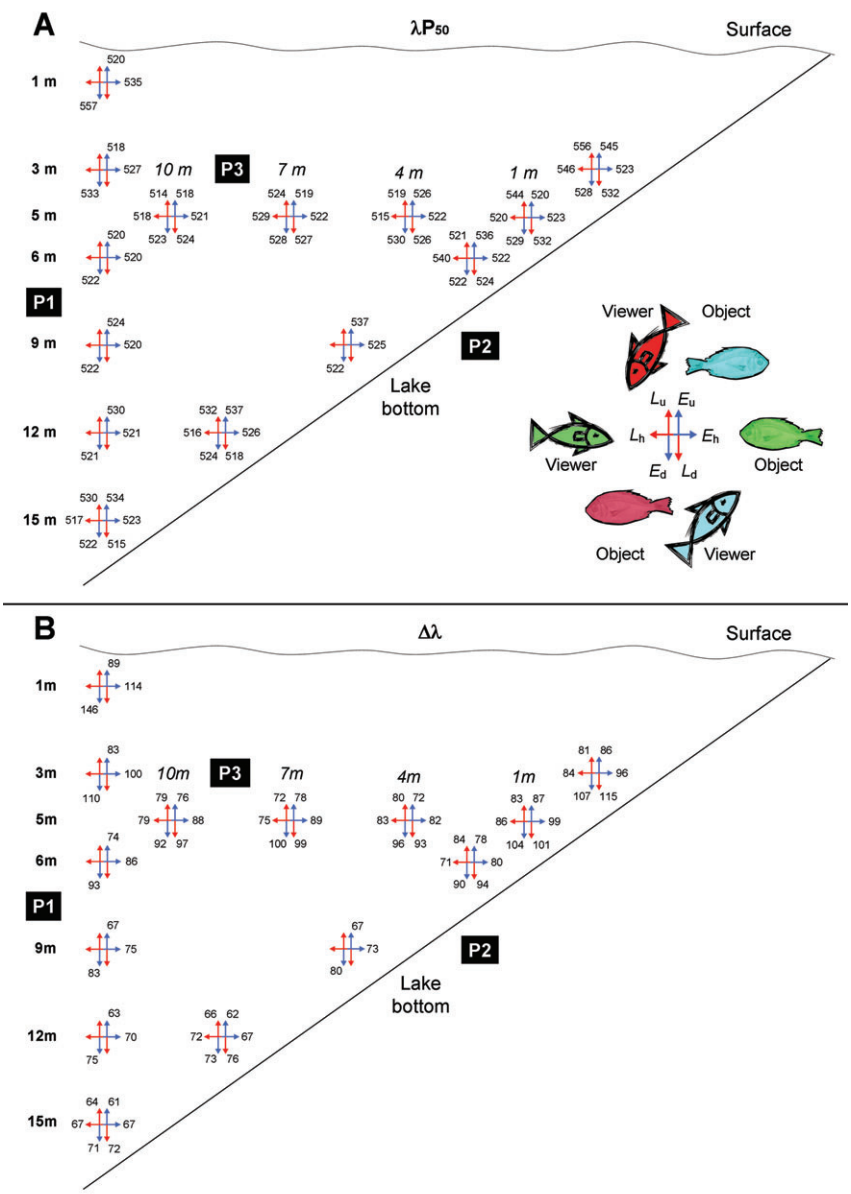

Fig. 8. A schematic representation of λP_{50} (A) and $\Delta\lambda$ (B) values calculated for all irradiance (blue) and radiance (red) spectra obtained in sand habitat in Lake Malawi. See Fig. 1 for conventions. Radiance was measured along P2 and P3 only.

orientation opposite to the one at which the irradiance illuminating the object is measured (Fig. 8A, inset). For example, when an object is viewed from above, it is illuminated by downwelling irradiance and viewed against the upwelling background radiance.

To examine the relationship between irradiance and radiance at opposite sampling orientations, irradiance–radiance pairs from both habitats were pooled. λP_{50} values of irradiance calculated for profile 2 differed significantly from those of radiance, whereas λP_{50} values of irradiance calculated for profile 3 did not differ significantly from those of radiance (Fig. 8A for the sand habitat and supplementary material Fig. S1A for the rock habitat; see supplementary material Table S3 for statistics). In general, $\Delta\lambda$ values of irradiance along both profiles differed significantly from those of radiance (Fig. 8B for the sand habitat and supplementary material Fig. S1B for the rock habitat; see supplementary material Table S3 for statistics). Therefore, irradiance and radiance at opposite orientations differed in their λP_{50} values when measured along the lake bottom (profile 2) but not when measured in the water column (profile 3).

Spectral beam attenuation

Water samples were collected in both habitats along the three measurement profiles. In all cases, the attenuation due to dissolved and particulate matter (c_{pg}) decreased with wavelength (Fig. 9). To evaluate the effect of the various environmental factors on the beam attenuation, the change in attenuation due to dissolved and particulate matter in the middle of the spectrum, 525 nm, was examined [$c_{pg}(525)$]. No significant correlations between $c_{pg}(525)$ and the water depth, bottom depth or proximity to the bottom were found. See supplementary material Table S2 for results of Spearman correlations to examine the effect of the various environmental factors on $c_{pg}(525)$. However, the attenuation measured along profile 3 in the rock habitat exhibited a bimodal dependence on the proximity to the bottom (Fig. 9), where sampling points farther from the bottom (2, 4 and 7 m from the bottom) showed significantly higher attenuation than points closer to the bottom (0.5 and 1 m from the bottom) (Mann–Whitney U-test, Z=–1.96, P<0.05, N=3). In general, however, the water was relatively homogeneous and no substantial differences in $c_{pg}(525)$ were found within each of the

Table 2. Effect of habitat and sampling orientation on the λP_{50} and $\Delta\lambda$ of irradiance and radiance

Quantity	Index	Effect	d.f.	F	P	Index value (nm)		
						E_d (sand)	E_h (rock)	E_u
Irradiance	λP_{50}	Habitat	1	29.1	**0.000**	526±7	515±11	
		Orientation	2	4.5	**0.014**	522±10	516±8	523±12
		Habitat × Orientation	2	0.7	0.481			
		Total	78					
	$\Delta\lambda$	Habitat	1	1.4	0.248	83±16	86±14	
		Orientation	2	10.1	**0.000**	94±18	84±12	76±10
		Habitat × Orientation	2	0.2	0.787			
		Total	78					
Radiance	λP_{50}	Habitat	1	0.1	0.705	527±10	527±9	
		Orientation	2	2.3	0.112	525±6	525±9	531±13
		Habitat × Orientation	2	0.0	0.987			
		Total	46					
	$\Delta\lambda$	Habitat	1	0.1	0.765	83±13	81±12	
		Orientation	2	7.1	**0.002**	91±14	77±8	79±11
		Habitat × Orientation	2	0.2	0.829			
		Total	46					

Results of multiple factorial ANOVAs. Data are means ± s.d. For the effect of habitat, index values for sand and rock habitats are given. For the effect of orientation, index values for the downwelling (E_d), sidewelling (E_h) and upwelling (E_u) directions are provided. Values in bold represent significant effects (P<0.05).

measurement profiles (rock habitat, profile 1: 0.200±0.032 m^{-1}, profile 2: 0.215±0.024 m^{-1}, profile 3: 0.476±0.193 m^{-1}; sand habitat, profile 1: 0.357±0.044 m^{-1}, profile 2: 0.515±0.052 m^{-1}, profile 3: 0.496±0.011 m^{-1}).

The magnitude of the beam attenuation varied across habitats. When all profiles in each habitat were pooled, $c_{pg}(525)$ in the sand habitat was significantly higher than that in the rock habitat. The $c_{pg}(525)$ in the sand habitat was higher when evaluating profiles 1 and 2 separately, but not when examining profile 3. See Table 4 for results of Mann–Whitney U-tests used to examine the effect of habitat on $c_{pg}(525)$. Additionally, the variation in $c_{pg}(525)$ within sites was higher in the rock habitat, with the coefficient of variation equal to 0.57 relative to 0.19 in the sand habitat, which is likely a result of the bimodal distribution along profile 3 in the rock habitat.

Next, to examine the effect of habitat on the shape of the spectral beam attenuation, the medians of the area-normalized shape of the attenuation spectra were compared (the average of the normalized shape is 1). The average spectral shape of c_{pg} differed between habitats, with higher short wavelength attenuation in the rock habitat (Fig. 10A), suggesting a variation in the characteristic of dissolved and particulate matter between habitats.

To evaluate the actual beam attenuation that the underwater radiance undergoes (which is relevant to an underwater observer), the total spectral beam attenuation, $c_t(\lambda)$, was calculated. Values of $c_t(\lambda)$ were highest at both ends of the spectrum examined (reaching 1.96 m^{-1} at 727 nm) and lowest at approximately 550 nm (Fig. 10B). Values of c_t in the sand habitat were larger than those in the rock habitat throughout the spectrum, being almost double in the middle of the spectrum (500–550 nm).

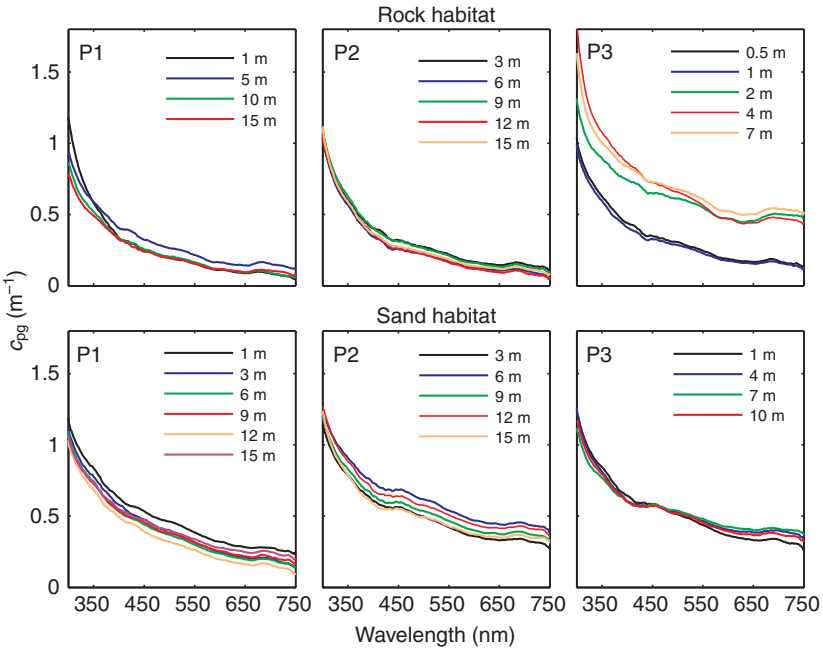

Fig. 9. Spectral beam attenuation due to dissolved and particulate matter, $c_{pg}(\lambda)$, along measurement profiles P1, P2 and P3 in rock and sand habitats in Lake Malawi.

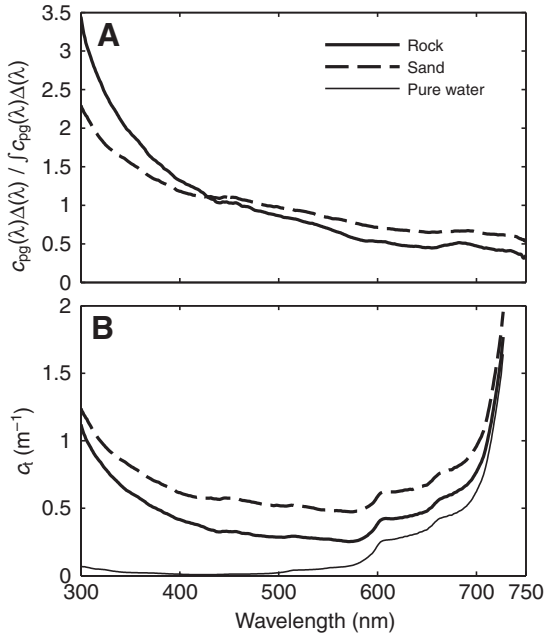

Fig. 10. Medians of the area-normalized shape of the spectral attenuation due to dissolved and particulate matter (A), and the median of the total spectral beam attenuation [$c_t(\lambda)$] (B) in rock and sand habitats in Lake Malawi. The beam attenuation of optically pure water is presented in B.

DISCUSSION

This study provides the first detailed description of the underwater photic conditions in Lake Malawi. Our analysis focuses on a comparison of two major habitat types, providing data that will be helpful for research aimed at understanding the visual biology, communication, behavior and ecology of cichlid species (data are available upon request).

In general, factors such as habitat type, water depth, bottom depth and proximity to the lake bottom all affected the irradiance and radiance distribution in the lake. The beam attenuation coefficient, however, was found to depend only on habitat type, at least at the two sites sampled. In the discussion below, the effects of the various environmental factors on the underwater photic environment will be summarized and the mechanisms underlying their effects will be evaluated. Finally, we will look at the implications for vision in cichlids by modeling the radiance contrast of various targets submerged in the rock and sand habitats, and the constraints imposed on the body color pattern of cichlids by the photic environment.

Effect of environmental factors on spectral irradiance, radiance and beam attenuation

Effect of habitat

Irradiance spectra in the sand-bottom habitat were significantly shifted to longer wavelengths compared with those in the rock-bottom habitat. However, the λP_{50} of radiance spectra did not differ significantly between habitats. The lack of dependence of the λP_{50} of downwelling radiance on habitat type is in agreement with our observation that the diffuse downwelling attenuation coefficient, K_d, differed between habitats mainly at short wavelengths (Fig. 5), where scattering is typically higher (Jerlov, 1976). By definition, irradiance accounts for light collected from a whole hemisphere and, as such, takes into account scattered light in the case of downwelling irradiance. Radiance, by contrast, accounts for light collected from a restricted acceptance angle (acceptance cone of 10 deg in this study) and, therefore, includes less scattered light when measuring downwelling radiance. Therefore, variation that occurs at short wavelengths is likely to be represented by downwelling irradiance rather than by downwelling radiance measurements. Close to the bottom, where downwelling light reflected from the bottom is prominent, the same mechanism applies to the upwelling direction. Another factor that may contribute to the lack of dependence of the λP_{50} of sidewelling and upwelling radiance on habitat type is the overall variation in radiance measurements due to spatial variation in the substrate included in the restricted angle sampled. The spectral bandwidth of both irradiance and radiance did not differ significantly between habitats.

Total beam attenuation in the sand habitat was higher than that in the rock habitat throughout the spectrum: almost double in the middle of the spectrum (500–550 nm). Attenuation was highest at both ends of the spectrum examined and lowest around 550 nm. Thus, in the context of visual communication, for example, the transmission of visual signals would be restricted to shorter distances in the sand habitat than in the rock habitat.

Effect of water depth

Descending the water column in the sand habitat, the spectra of downwelling and sidewelling irradiance shifted to shorter wavelengths down to approximately 6 m. Moving deeper, however, where not much long-wavelength light remains, the relative contribution of attenuation at short wavelengths increased and the spectra shifted to longer wavelengths (Fig. 3 and Fig. 4A for both

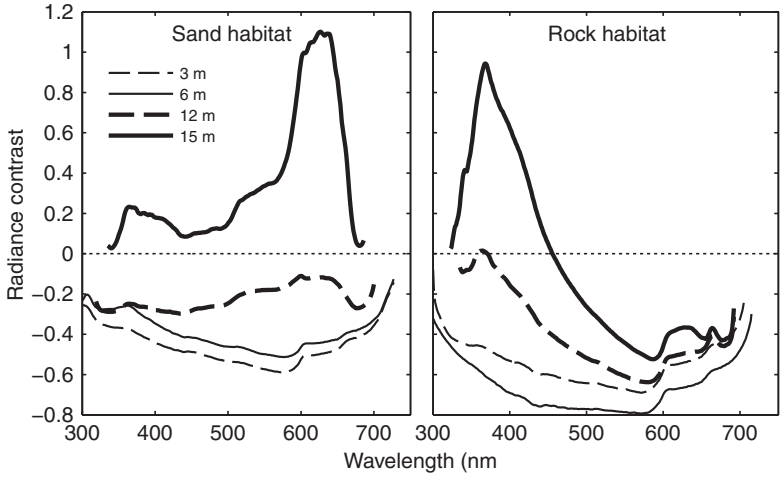

Fig. 11. Radiance contrast of a target reflecting 20% of impinging irradiance uniformly across the spectrum, as viewed from 1 m away, at various depths in sand and rock habitats in Lake Malawi.

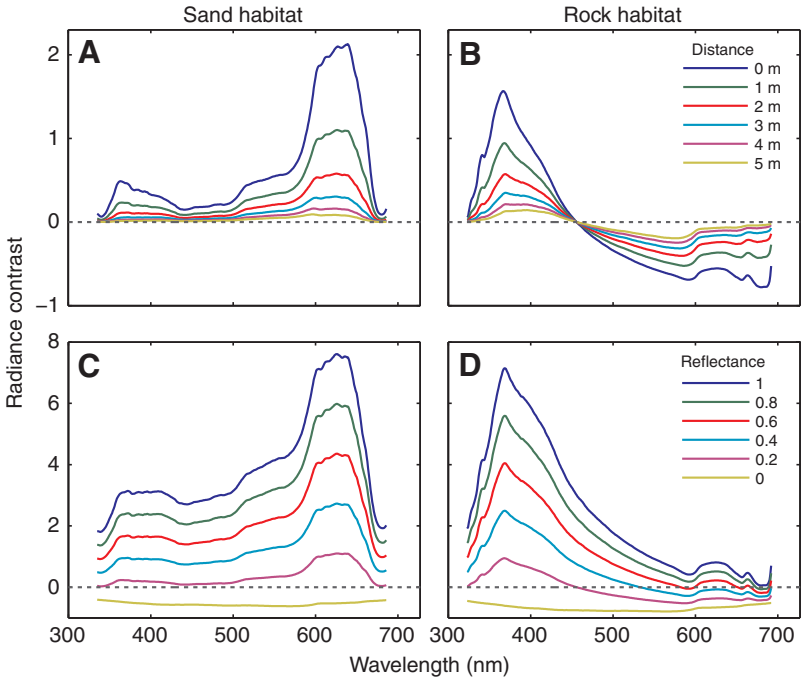

Fig. 12. Radiance contrast at variable distances away from a target (A,B) and of targets of variable reflectance (C,D) for targets at 15 m depth in sand (A,C) and rock (B,D) habitats in Lake Malawi.

habitats). The transition depth between these two trends is likely dependent on the interplay between the attenuation due to particulate and dissolved matter at short wavelengths, and the attenuation due to water molecules at long wavelengths (Jerlov, 1976). Therefore, different transition depths would be expected at different sites that vary in water constituents. Indeed, the sand habitat, where attenuation at short wavelengths was higher, showed a shallower transition depth than the rock habitat (Fig. 3).

Depending on the spectral reflectance of the substrate, downwelling irradiance incident on a reflective substrate tends to produce a broader and long-wavelength-shifted spectrum relative to that of the upwelling irradiance and radiance (McFarland and Munz, 1975). Thus, when descending the water column and approaching the lake bottom, upwelling irradiance spectra shift to longer wavelengths. Interestingly, the magnitude of this long-wavelength shift of the upwelling spectra was larger in the sand habitat, suggesting that a larger proportion of long-wavelength light was reflected from sand than from rock substrate (Fig. 3). It is important to note, however, that other habitats with different substrates (e.g. sand particles of different sizes and colors or rocks covered with different types of algae and organic matter) may affect the upwelling irradiance differently.

The spectral bandwidth of irradiance significantly decreased with depth at all sampling orientations (Fig. 4D–F), with the spectra of downwelling irradiance exhibiting the largest bandwidth, those of upwelling irradiance exhibiting the smallest bandwidth and those of sidewelling irradiance exhibiting intermediate spectral bandwidth. The decrease in spectral bandwidth with depth was a result of the high attenuation at short and long wavelengths that narrowed the spectrum. The variation in spectral bandwidth across the three sampling orientations correlated negatively with the path length of photons through the water column.

Effect of bottom depth

Maintaining a constant distance to the bottom, sidewelling and upwelling irradiance were expected to depend on both bottom reflections that were dominated by long wavelengths and the downwelling irradiance impinging on the bottom that was dominated

Table 3. Total irradiance measured along profile 1 and total radiance measured along profile 2 in sand and rock habitats

Quantity	Habitat	Orientation	Surface	Min. depth	Max. depth
Total irradiance (photons cm^{-2} s^{-1})	Sand	D	1.74E+17	5.80E+16	5.23E+15
		H		1.21E+16	1.15E+15
		U		1.24E+15	2.45E+14
	Rock	D	1.08E+17	8.02E+16	6.37E+15
		H		2.99E+15	6.2E+14
		U		7.43E+14	1.29E+14
Total radiance (photons cm^{-2} sr^{-1} s^{-1})	Sand	D	2.01E+17	1.27E+16	5.05E+15
		H		2.38E+15	1.57E+15
		U		5.61E+14	2.42E+14
	Rock	D	2.7E+16	2.5E+16	5.2E+15
		H		1.7E+15	1.9E+14
		U		6.8E+14	–

Irradiance/radiance were integrated between 300 and 750 nm. Total irradiance/radiance is provided for just above the surface and at the minimum and maximum measurement depths for downwelling (D), sidewelling (H) and upwelling (U) sampling orientations. The minimum measurement depth of irradiance was 1 m whereas the minimum measurement depth of radiance was 3 m. The maximum measurement depth for both quantities was 15 m. For reference, see Table 1 for the specific solar zenith angles under which irradiance and radiance were measured.

Table 4. Summary of the results of Mann–Whitney *U*-tests used for the examination of the effect of habitat on the attenuation due to dissolved and particulate matter, $c_{pg}(525)$

Profile	*N*	*Z*	*P*	$c_{pg}(525)$ (m^{-1})	
				Sand	Rock
1	9	0.49	0.624	0.357±0.044	0.200±0.033
2	10	–2.61	**0.008**	0.515±0.053	0.216±0.024
3	10	–2.56	**0.009**	0.496±0.011	0.476±0.193
All	29	–2.66	**0.007**	0.447±0.085	0.304±0.172

Data are means ± s.d. Values in bold represent significant effects (P<0.05).

by spectra shifted to shorter wavelengths with depth. Indeed, when descending along the bottom (profile 2), apart from an initial shift of the upwelling irradiance spectra to short wavelengths, the λP_{50} of both upwelling and sidewelling irradiance spectra did not vary with depth. Additionally, upwelling irradiance spectra were always shifted to longer wavelengths than those at other sampling orientations. The spectral bandwidth of irradiance decreased with depth at all sampling orientations.

For radiance, downwelling and sidewelling spectra shifted to shorter wavelengths with depth. However, the λP_{50} of upwelling radiance spectra did not depend on depth. The spectral bandwidth of downwelling radiance decreased with depth whereas those of sidewelling and upwelling radiance did not. Radiance, sampled over a restricted angle, is sensitive to variation in the bottom substrate, algae cover and any physical interference along the line of sight, supporting the lack of depth dependence for sidewelling and upwelling but not for downwelling radiance.

Effect of proximity to bottom

Downwelling irradiance spectra did not change in bandwidth or exhibit spectral shifting while moving away from shore at a constant water depth of 5 m, suggesting that the lake water was spatially homogeneous at this depth. The slight variation observed was likely a result of the rugged topography in the rock habitat, where large boulders were scattered along the bottom, possibly creating patches of varying water turbidity. This variation was not apparent in the sand habitat, where the bottom was more uniform.

Bottom reflections were expected to increase the proportion of long wavelengths in the water column, when viewed from above. Because of a decreasing contribution of bottom reflections, upwelling irradiance and, to a lesser extent, sidewelling irradiance were expected to shift to shorter wavelengths with increasing distance from the bottom. Indeed, upwelling spectra narrowed and shifted to short wavelengths with increasing distance away from the bottom (Fig. 4C,F). In contrast, sidewelling spectra did not depend on the distance to the bottom, likely a result of the high downwelling irradiance masking the contribution of the relatively low intensity bottom reflections.

Similar to irradiance, upwelling radiance spectra shifted to short wavelengths with increasing distance from the lake bottom, whereas downwelling radiance spectra did not vary with distance from the lake bottom. Contrary to the trend observed for irradiance, sidewelling radiance spectra shifted to short wavelengths with distance from the bottom. This is due to the small contribution of downwelling radiance to the sidewelling radiance sampled (as opposed to the case of irradiance). Downwelling radiance spectra exhibited larger spectral bandwidths than those of sidewelling and upwelling radiance (Fig. 7D). Our results demonstrate the effect of bottom reflections on the upwelling and sidewelling irradiance and radiance up to 7 m away from the bottom. Thus, the influence of bottom reflections was notable and their contribution to the irradiance and radiance fields should be considered.

Comparison of the photic environment of tropical Lake Malawi with tropical seas

It is reasonable and useful to compare the photic environment of the oligotrophic Lake Malawi with that of tropical seas (McFarland and Munz, 1975). Similar to Lake Malawi cichlids, coral reef fishes have some of the most striking and diverse color patterns (Marshall, 2000; Marshall et al., 2003a; Marshall et al., 2003b; Marshall et al., 2006); thus, comparing the photic environments of these two ecosystems, which have favored the evolution of fish color (and presumably vision), is interesting. In agreement with our findings, λP_{50} and $\Delta\lambda$ of downwelling irradiance measured offshore the Kona coast in Hawaii decreased with depth (McFarland and Munz, 1975). However, λP_{50} values in Lake Malawi (523–522 nm and 514–508 nm at 5–15 m depth in the sand and rock habitats, respectively) were longer than those obtained for the tropical sea (518–492 nm; at 5–15 m depth). $\Delta\lambda$ values for Lake Malawi (97–71 nm in both habitats) were smaller than those for the tropical sea (102–82 nm; at 5–15 m depth), indicating a stronger attenuation at both ends of the spectrum in Lake Malawi. Additionally, the qualitative effects of water depth and proximity to the bottom on radiance in Lake Malawi agree with those for the tropical sea (McFarland and Munz, 1975). Thus, although the irradiance spectra from Lake Malawi were narrower and shifted to longer wavelengths than those in the tropical sea, the processes shaping the irradiance and radiance fields were qualitatively similar in both ecosystems.

Lake Malawi photic environment and its implications for fish vision

Spectral radiance contrast

We estimated the spectral radiance contrast of cichlids in order to identify the forces that might have shaped their color patterns and visual systems. To estimate the radiance contrast of fish in different positions in the sand and rock habitats, we calculated the radiance contrast of various targets using the sidewelling irradiance and radiance and beam attenuation data collected while descending along the lake bottom (profile 2). Note that the virtual targets were perfectly flat and vertical in orientation. First, the radiance contrast (C) was calculated for a hypothetical target diffusely reflecting 20% of incident irradiance uniformly across the spectrum (R=0.2; 300–727 nm), viewed from 1 m away (Fig. 11). A reflectance of 20% was chosen to approximate the reflectance from the body patterns of Malawi cichlids (S.S., S.M.G., C.W.H., unpublished). It is important to note that the actual radiance reflected from a fish in its natural habitat will depend heavily on its bidirectional reflectance distribution function; because the fish body is typically curved (as seen in cross-section), it is illuminated from multiple directions and may also exhibit some specular reflection.

The spectral range over which the radiance contrast of a spectrally uniform target is highest is an attribute of the photic environment and does not depend on the spectral reflectance properties of the object in any way. However, this spectral range is where any object would attain the highest possible radiance contrast (ideal spectral range). Therefore, to attain the highest possible radiance contrast and to be the most conspicuous, Malawi cichlids are expected to have body color patterns that preferentially reflect radiance over this ideal spectral range. In addition and independently of the reflectance properties of the fish color pattern, cichlids are expected to show high visual sensitivity over this ideal spectral range in order to perceive the highest possible radiance contrast of other cichlids.

In both habitats, the radiance contrast at 3, 6 and 12 m depth (shallow water) was negative, whereas at 15 m depth (deep water) the radiance contrast was mostly positive (Fig. 11). Thus, in shallow water, target radiance was lower than the background radiance, whereas in deep water target radiance was higher than the background radiance. In shallow water, the radiance contrast was relatively flat across the spectrum, whereas in deep water, radiance contrast varied considerably across the spectrum with the two habitats differing in the spectral region over which the maximum contrast was evident. Radiance contrast at depth was maximal at long wavelengths (600–650 nm) in the sand habitat, and at short wavelengths (350–400 nm) in the rock habitat.

The radiance contrast was also calculated for targets exhibiting variable reflectance (R=0–1) and viewed from different distances (z=0–5 m) when submerged at 15 m depth, a depth that is often occupied by many cichlid species (see supplementary material Table S4 and references within for depth distribution of various cichlid species). In both habitats, radiance contrast decreased with increasing distance to the viewer and decreasing target reflectance (Fig. 12). Although the background radiance does not depend on the distance to the viewer, the target radiance attenuates and becomes similar to the background radiance with increasing distance and a reduction in reflectance. Importantly, regardless of the distance to the target and its reflectance, the radiance contrast was maximal at long wavelengths in the sand habitat and at short wavelengths in the rock habitat.

Constraints imposed on the color pattern of cichlids

Based on the effects of habitat and depth on the radiance contrast of cichlids, the color patterns of sand- and rock-dwelling cichlids that reside in deep water, and less so in shallow water, are expected to be restricted to certain spectral regions to achieve optimal radiance contrast. To achieve the highest conspicuousness, the color patterns of rock-dwelling cichlids should be restricted to short wavelengths whereas those of sand-dwelling cichlids should be restricted to long wavelengths.

Cichlids from different habitats exhibit different bar/stripe patterns. Bar patterns are typically found in cichlids associated with structurally complex habitats (including rocky habitats) whereas horizontal stripes are more often associated with shoaling behavior, which is typical for open-water and sand-dwelling cichlids (Seehausen et al., 1999). The color pattern of Malawi cichlids was previously characterized by Deutsch (Deutsch, 1997) and McElroy (McElroy, 1991). However, both studies relied on human visual inspection of photographs and thus have limited significance for understanding the spectral reflectance of cichlids. Recently, the spectral reflectance of several rock-dwelling cichlids was reported (Dalton et al., 2010; Jordan et al., 2004) and showed high conspicuousness of males but not of females under natural conditions (Dalton et al., 2010). To date, however, there has been no comparative investigation aimed at characterizing the spectral reflectance of sand- and rock-dwelling cichlids. Such an analysis would contribute to our understanding of the evolution of color patterns in Lake Malawi cichlids and test the predictions presented here.

Constraints imposed on the visual system of cichlids

Rock- and sand-dwelling cichlids possess a similar set of cone opsin genes that encode seven spectrally distinct cone pigments that can be differentially expressed (Carleton and Kocher, 2001; Hofmann et al., 2009; Parry et al., 2005; Sabbah et al., 2010b). This raises an interesting question: is the visual system of cichlids tuned to their photic environment to allow for conspicuousness of color patterns in conspecific cichlids? In fact, in a recent report, Sabbah et al. (Sabbah et al., 2010b) have shown that the visual sensitivity of cichlids correlated with the level of long-wavelength radiance reflected from the body of conspecifics under natural photic conditions.

The highest possible radiance contrast in the sand habitat was evident at long wavelengths. Thus, a long-wavelength-shifted visual system would enhance the detection capabilities of sand-dwelling cichlids. This prediction relies on the offset hypothesis originally put forth by Lythgoe (Lythgoe, 1968), where detection capabilities would be enhanced by using a visual pigment with a λ_{max} offset from the background to produce the highest possible radiance contrast. In fact, sand-dwellers have been shown to express opsin genes that encode visual pigments sensitive to wavelengths longer than those expressed by rock-dwellers and pelagic species (Hofmann et al., 2009).

To investigate the effect of depth on opsin gene expression of rock- and sand-dwelling cichlids, we reanalyzed the opsin gene expression data from Hofmann et al. (Hofmann et al., 2009). To do this, we roughly grouped cichlid species into shallow-water and deep-water species; species with depth ranges shallower than 10 m were considered shallow-water species whereas those with depth ranges deeper than 10 m were considered deep-water species, even if they are also found at shallow depths (supplementary material Table S4). We performed multiple ANOVA tests where an experiment-wise error rate of 5% was corrected to 0.0083 (α=0.05/6=0.0083) following Bonferroni correction for six hypothesis tests (Quinn and Keough, 2002) corresponding to six opsin genes [RH2aα and RH2aβ were pooled because of genetic and functional similarity (Parry et al., 2005; Spady et al., 2006)]. The expression of the long-wavelength-sensitive (LWS) opsin gene was significantly higher in sand-dwelling cichlids and in deep-water species. *Post hoc* analysis revealed that the expression of LWS in sand-dwelling cichlids was significantly higher than that in rock-dwelling cichlids residing in deep water (P=0.0004, N=26) but not in shallow water (P=0.998). The expression of all other cone opsin genes did not depend on habitat type and depth. See supplementary material Table S5 for a summary of ANOVA results. Thus, the expression of LWS was similar across habitats in shallow water whereas in deep water, the expression of LWS in sand-dwellers was higher than in rock-dwellers. This analysis suggests that the visual system of cichlids is tuned to provide the highest possible radiance contrast in deep water.

Effect of the context of visual communication on radiance contrast

It is important to consider the context in which visual communication takes place when evaluating the radiance contrast of fish. For example, in mate choice, rock-dwelling females choose between males that typically defend territories between rocks. Males typically

perform visual displays to females against the background of a rock. In this situation, the male is illuminated by sidewelling irradiance oriented towards the rock background, and is viewed against the background sidewelling radiance coming from the direction of the rock. A similar visual context applies to male–male competition situations. In this study, irradiance and radiance measured at opposite orientations differed in λP_{50} when measured along the lake bottom (profile 2) but not when measured in the water column (profile 3). Therefore, in order to achieve the optimal radiance contrast, fish occupying different habitats and assuming different positions within each habitat would be expected to differ in their spectral reflectance and the spectral tuning of their visual system.

CONCLUSIONS

Key findings

1. Irradiance spectra were shifted to longer wavelengths and total beam attenuation was higher in the sand habitat compared with those in the rock habitat.
2. Descending in the water column, downwelling and sidewelling irradiance spectra shifted to shorter wavelengths whereas upwelling irradiance spectra shifted to longer wavelengths because of a high contribution of bottom reflections.
3. The irradiance–radiance relationship in the water column differed from that along the bottom; thus, to achieve conspicuousness, the body reflectance and visual system of cichlids occupying different positions within each habitat would be constrained differently.
4. To achieve conspicuousness, the color patterns of rock- and sand-dwelling cichlids would be constrained to short and long wavelengths, respectively.
5. In shallow water, the expression of the LWS opsin gene was similar across clades whereas in deep water, the expression of LWS in sand-dwelling cichlids was higher than in rock-dwelling cichlids, suggesting that the visual systems of cichlids are tuned to provide the highest possible radiance contrast in their photic environment.

ACKNOWLEDGEMENTS

The authors thank the University of Malawi and the personnel at the Mbuna Research Station, Cape Maclear, Malawi, and Drs Tom Kocher and Karen Carleton for helpful suggestions regarding the selection of the study sites. This research was supported by a Natural Sciences and Engineering Research Council of Canada (NSERC) Discovery Grant and an NSERC Research Tools and Instrumentation Grant, the Canada Foundation for Innovation, the Ontario Innovation Trust and the Canada Research Chair Program (C.W.H.). S.S. was supported by a Vanier Canada Graduate Scholarship from NSERC. S.M.G. was supported by an NSERC Postdoctoral Fellowship.

REFERENCES

Bootsma, H. A. and Hecky, R. E. (2003). A comparative introduction to the biology and limnology of the African Great Lakes. *J. Great Lakes Res.* **29**, 3-18.
Carleton, K. L. and Kocher, T. D. (2001). Cone opsin genes of African cichlid fishes: tuning spectral sensitivity by differential gene expression. *Mol. Biol. Evol.* **18**, 1540-1550.
Carleton, K. L., Spady, T. C. and Kocher, T. D. (2006). Visual communication in East Africa cichlid fishes: diversity in a phylogenetic context. In *Communication in Fishes* (ed. F. Ladich, S. P. Collin, P. Moller and B. G. Kapoor), pp. 481-511. Enfield, NH: Science Publishers.
Couldridge, V. C. K. and Alexander, G. J. (2002). Color patterns and species recognition in four closely related species of Lake Malawi cichlid. *Behav. Ecol.* **13**, 59-64.
Dalton, B. E., Cronin, T. W., Marshall, N. J. and Carleton, K. L. (2010). The fish eye view: are cichlids conspicuous? *J. Exp. Biol.* **213**, 2243-2255.
Deutsch, J. C. (1997). Colour diversification in Malawi cichlids: evidence for adaptation, reinforcement or sexual selection? *Biol. J. Linn. Soc.* **62**, 1-14.
Duntley, S. Q. (1962). Underwater visibility. In *The Sea, Physical Oceanography*, vol. 1 (ed. M. N. Hill), pp. 452-455. New York: Wiley.
Duntley, S. Q. (1963). Light in sea. *J. Opt. Soc. Am.* **53**, 214-233.
Endler, J. A., Westcott, D. A., Madden, J. R. and Robson, T. (2005). Animal visual systems and the evolution of color patterns: sensory processing illuminates signal evolution. *Evolution* **59**, 1795-1818.
Fryer, G. and Iles, T. D. (1972). *The Cichlid Fishes of the Great Lakes of Africa: Their Biology and Evolution*. Neptune City, NJ: T. F. H. Publications.
Halfman, J. D. and Scholz, C. A. (1993). Suspended sediments in Lake Malawi, Africa – a reconnaissance study. *J. Great Lakes Res.* **19**, 499-511.
Hawryshyn, C. W. and Harosi, F. I. (1994). Spectral characteristics of visual pigments in rainbow trout (*Oncorhynchus mykiss*). *Vision Res.* **34**, 1385-1392.
Hofmann, C. M., O'Quin, K. E., Marshall, N. J., Cronin, T. W., Seehausen, O. and Carleton, K. L. (2009). The eyes have it: regulatory and structural changes both underlie cichlid visual pigment diversity. *PLoS Biol.* **7**. Epub e1000266.
Jerlov, N. G. (1976). *Marine Optics*. Amsterdam: Elsevier.
Jordan, R., Kellogg, K., Juanes, F. and Stauffer, J. (2003). Evaluation of female mate choice cues in a group of Lake Malawi mbuna (Cichlidae). *Copeia* **2003**, 181-186.
Jordan, R., Howe, D., Juanes, F., Stauffer, J. and Loew, E. (2004). Ultraviolet radiation enhances zooplanktivory rate in ultraviolet sensitive cichlids. *Afr. J. Ecol.* **42**, 228-231.
Kelber, A., Vorobyev, M. and Osorio, D. (2003). Animal colour vision – behavioural tests and physiological concepts. *Biol. Rev.* **78**, 81-118.
Kirk, J. T. O. (1981). Monte Carlo study of the nature of the underwater light field in, and the relationships between optical properties of, turbid yellow waters. *Aust. J. Mar. Fresh. Res.* **32**, 517-532.
Konings, A. (1995). *Lake Malawi Cichlids in their Natural Habitat*. El Paso, TX, USA: Cichlid Press.
Losey, G. S., McFarland, W. N., Loew, E. R., Zamzow, J. P., Nelson, P. A. and Marshall, N. J. (2003). Visual biology of Hawaiian coral reef fishes. I. Ocular transmission and visual pigments. *Copeia* **2003**, 433-454.
Lu, Z. (2006). Optical Absroption of Pure Water in the Blue and Ultraviolet. PhD Thesis, pp. 100, Texas A&M University, College Station, TX.
Lythgoe, J. N. (1968). Visual pigments and visual range underwater. *Vision Res.* **8**, 997-1012.
Marshall, N. J. (2000). Communication and camouflage with the same 'bright' colours in reef fishes. *Philos. Trans. R. Soc. Lond. B Biol. Sci.* **355**, 1243-1248.
Marshall, N. J., Jennings, K., McFarland, W. N., Loew, E. R. and Losey, G. S. (2003a). Visual biology of Hawaiian coral reef fishes. II. Colors of Hawaiian coral reef fish. *Copeia* **2003**, 455-466.
Marshall, N. J., Jennings, K., McFarland, W. N., Loew, E. R. and Losey, G. S. (2003b). Visual biology of Hawaiian coral reef fishes. III. Environmental light and an integrated approach to the ecology of reef fish vision. *Copeia* **2003**, 467-480.
Marshall, N. J., Vorobyev, M. and Siebeck, U. E. (2006). What does a reef fish see when it sees a reef fish? Eating "Nemo"©. In *Communication in Fishes*, vol. 2 (ed. F. Ladich, S. Collin, P. Moller and B. G. Kapoor), pp. 393-422. Enfield, NH: Science Publishers.
McElroy, D. M., Kornfield, I. and Everett, J. (1991). Coloration in African cichlids – Diversity and constraints in Lake Malawi endemics. *Neth. J. Zool.* **41**, 250-268.
McFarland, W. N. and Munz, F. W. (1975). Part II: the photic environment of clear tropical seas during the day. *Vision Res.* **15**, 1063-1070.
Mobley, C. D. (1994). *Light and Water*. San Diego, CA: Academic Press.
Parry, J. W. L., Carleton, K. L., Spady, T., Carboo, A., Hunt, D. M. and Bowmaker, J. K. (2005). Mix and match color vision: Tuning spectral sensitivity by differential opsin gene expression in Lake Malawi cichlids. *Curr. Biol.* **15**, 1734-1739.
Pilskaln, C. H. and Johnson, T. C. (1991). Seasonal signals in Lake Malawi sediments. *Limnol. Oceanogr.* **36**, 544-557.
Pope, R. M. and Fry, E. S. (1997). Absorption spectrum (380-700 nm) of pure water. 2. Integrating cavity measurements. *Appl. Opt.* **36**, 8710-8723.
Quinn, G. P. and Keough, M. J. (2002). *Experimental Design and Data Analysis for Biologists*. New York: Cambridge University Press.
Ribbink, A. J., Marsh, B. A., Marsh, A. C., Ribbink, A. C. and Sharp, B. J. (1983). A preliminary survey of the cichlid fishes of rocky habitats in Lake Malawi. *S. Afr. J. Zool.* **18**, 149-310.
Sabbah, S., Fraser, J. M., Boss, E. S., Blum, I. and Hawryshyn, C. W. (2010a). Hyperspectral portable beam transmissometer for the ultraviolet-visible spectrum. *Limnol. Oceanogr. Methods* **8**, 527-538
Sabbah, S., Lamela Laria, R., Gray, S. M. and Hawryshyn, C. W. (2010b). Functional diversity in the color vision of cichlid fishes. *BMC Biol.* **8**, 133.
Salzburger, W. (2009). The interaction of sexually and naturally selected traits in the adaptive radiations of cichlid fishes. *Mol. Ecol.* **18**, 169-185.
Scott, W. B. and Crossman, E. J. (1973). Freshwater fishes of Canada. *Bull. Fish. Res. Board Canada* **184**, 966.
Seehausen, O. and van Alphen, J. J. M. (1998). The effect of male coloration on female mate choice in closely related Lake Victoria cichlids (*Haplochromis nyererei* complex). *Behav. Ecol. Sociobiol.* **42**, 1-8.
Seehausen, O., van Alphen, J. J. M. and Witte, F. (1997). Cichlid fish diversity threatened by eutrophication that curbs sexual selection. *Science* **277**, 1808-1811.
Seehausen, O., Mayhew, P. J. and Van Alphen, J. J. M. (1999). Evolution of colour patterns in East African cichlid fish. *J. Evol. Biol.* **12**, 514-534.
Seehausen, O., Terai, Y., Magalhaes, I. S., Carleton, K. L., Mrosso, H. D. J., Miyagi, R., van der Sluijs, I., Schneider, M. V., Maan, M. E., Tachida, H. et al. (2008). Speciation through sensory drive in cichlid fish. *Nature* **455**, 620-626.
Spady, T. C., Parry, J. W. L., Robinson, P. R., Hunt, D. M., Bowmaker, J. K. and Carleton, K. L. (2006). Evolution of the cichlid visual palette through ontogenetic subfunctionalization of the opsin gene arrays. *Mol. Biol. Evol.* **23**, 1538-1547.
Underwood, A. J. (1997). *Experiments in Ecology*. Cambridge, UK: Cambridge University Press.
Vorobyev, M., Osorio, D., Bennett, A. T. D., Marshall, N. J. and Cuthill, I. C. (1998). Tetrachromacy, oil droplets and bird plumage colours. *J. Comp. Physiol. A,* **183**, 621-633.
Voss, K. J. and Austin, R. W. (1993). Beam-attenuation measurement error due to small-angle scattering acceptance. *J. Atmos. Ocean. Technol.* **10**, 113-121.
Zhang, X. D., Hu, L. B. and He, M. X. (2009). Scattering by pure seawater: Effect of salinity. *Opt. Express* **17**, 5698-5710.